The RNA exosome affects iron response and sensitivity to oxidative stress

BORISLAVA TSANOVA,[1] PHYLLIS SPATRICK,[2] ALLAN JACOBSON,[2] and AMBRO VAN HOOF[1,3]

[1]Department of Microbiology and Molecular Genetics, University of Texas Health Science Center–Houston and The University of Texas Graduate School of Biomedical Sciences, Houston, Texas 77030, USA
[2]Department of Microbiology and Physiological Systems, Albert Sherman Center, University of Massachusetts Medical School, Worcester, Massachusetts 01655, USA

ABSTRACT

RNA degradation plays important roles for maintaining temporal control and fidelity of gene expression, as well as processing of transcripts. In *Saccharomyces cerevisiae* the RNA exosome is a major 3′-to-5′ exoribonuclease and also has an endonuclease domain of unknown function. Here we report a physiological role for the exosome in response to a stimulus. We show that inactivating the exoribonuclease active site of Rrp44 up-regulates the iron uptake regulon. This up-regulation is caused by increased levels of reactive oxygen species (ROS) in the mutant. Elevated ROS also causes hypersensitivity to H_2O_2, which can be reduced by the addition of iron to H_2O_2 stressed cells. Finally, we show that the previously characterized slow growth phenotype of *rrp44-exo*$^-$ is largely ameliorated during fermentative growth. While the molecular functions of Rrp44 and the RNA exosome have been extensively characterized, our studies characterize how this molecular function affects the physiology of the organism.

Keywords: DIS3; RNA degradation; RRP44; yeast

INTRODUCTION

The exosome is a major exoribonuclease found in eukaryotes and archaea (Mitchell et al. 1997; Allmang et al. 1999b; Chekanova et al. 2002; Evguenieva-Hackenberg et al. 2003). In eukaryotes, including *Saccharomyces cerevisiae*, the exosome is a complex of 10 essential proteins, which in addition to its exonuclease activity also has an endonuclease activity (Lebreton et al. 2008; Schaeffer et al. 2009; Schneider et al. 2009). These catalytic activities are carried out by separate domains of the Rrp44 protein. The exosome is known to be located both in the nucleus and in the cytoplasm. In the nucleus it takes part of 3′ processing of the 5.8S rRNA, snoRNAs, snRNAs, and some mRNAs (Mitchell et al. 1996; Allmang et al. 1999a; van Hoof et al. 2000). It also degrades the 5′ external transcribed spacer (ETS) of rRNA, misprocessed RNAs such as hypomodified tRNA, and cryptic unstable transcripts (CUTs) (Kadaba et al. 2004; Milligan et al. 2008). In the cytoplasm, the exosome takes part in the degradation of normal, as well as aberrant, mRNAs (Jacobs Anderson and Parker 1998; van Hoof et al. 2002; Meaux and van Hoof 2006). Most of the activities of the exosome require the exoribonuclease activity of Rrp44, while the function of its endonuclease activity is enigmatic (Lebreton et al. 2008; Schaeffer et al. 2009; Schneider et al. 2009; Schaeffer and van Hoof 2011).

Studies of Rrp44's physiological function are limited. Rrp44 was shown to affect chromosome segregation, cell cycle progressions, and microtubules in *Schizosaccharomyces pombe* and *S. cerevisiae* (Murakami et al. 2007; Smith et al. 2011). Rrp44 has also been found to alter the circadian rhythm in *Neusporra crassa* (Guo et al. 2009). How any of these effects are related to the catalytic activities of Rrp44 is unknown. In addition to studies on Rrp44, it has been shown that the exosome components Rrp4 and Rrp41 have specific roles during early development of *Arabidopsis thaliana* (Chekanova et al. 2007). Here we characterize the effect of the catalytic activities of the exosome on the physiology of *S. cerevisiae* and find effects related to reactive oxygen species (ROS), iron uptake, and carbon utilization.

Iron is an essential element that functions in cellular metabolism because of its ability to be easily converted between oxidized and reduced forms, thus being a readily available electron donor or recipient. It is critical to maintain the precise balance of iron concentration inside the cell. Insufficient iron will adversely affect cellular metabolism since iron is a

[3]**Corresponding author**
E-mail Ambro.van.hoof@uth.tmc.edu

Article published online ahead of print. Article and publication date are at http://www.rnajournal.org/cgi/doi/10.1261/rna.043257.113.

cofactor in many enzymatic reactions. Conversely, too much free iron is toxic to the cell because it takes part in the formation of damaging hydroxyl radical species through the Fenton reaction and leads to oxidative stress. Oxidative stress in turn has been known to damage all cellular components, including lipids, DNA, RNA, and proteins and in humans is related to several diseases, including neurodegenerative diseases such as ALS; Alzheimer's, Huntington's, and Parkinson's disease; and plaque formation in the arteries. It is also a contributing factor in the aging process (Trushina and McMurray 2007; Brieger et al. 2012; Chen and Keaney 2012; Gomez-Cabrera et al. 2012).

When yeast senses that its iron level is insufficient, it up-regulates the master regulator of iron response, Aft1, which then binds to the promoter of genes required for iron uptake and induces their transcription (Crisp et al. 2003; Rutherford et al. 2005). The exact signal that is sensed and transduced to Aft1 is unknown, but it results in relocalization of Aft1. Under iron replete conditions. Aft1 localizes to the cytoplasm, while activation of Aft1 causes its relocalization to the nucleus (Yamaguchi-Iwai et al. 1996, 2002).

As mentioned above, inappropriately high iron level causes production of ROS. Under normal iron levels, respiration is the major contributor to ROS production by electrons leaking from the electron transport chain (Herrero et al. 2008). During growth on glucose, *S. cerevisiae* suppresses the genes for respiration and grows by fermentation. When glucose is no longer available, it switches to respiration and oxidizes the remaining nonfermentable carbon source.

Here we show that inactivation of the exoribonuclease activity of the exosome results in the reduced ability of the cell to resist oxidative stress and up-regulates the iron uptake response. Moreover, we show that these effects and the significant growth defect of this strain are present during fermentative growth but not during respiratory growth. Overall, these results demonstrate that the molecular function of the exosome affects the physiology of the organism.

RESULTS AND DISCUSSION

Activation of the iron-starvation response is a major physiological consequence of a defect in Rrp44 exonuclease activity

We used microarray analysis to characterize the physiological effects of inactivating either the endoribonuclease or the exoribonuclease activity of the exosome. Specifically, we isolated polyadenylated RNA from quadruplicate cultures of wild type and two *rrp44* mutants that have previously been characterized. The *rrp44-exo*$^-$mutation changes Asp551 of the exonuclease active site to Asn, disrupts the exonuclease activity, and results in many RNA processing and degradation defects (Dziembowski et al. 2007). Importantly, although the exonuclease acts in mRNA decay, it only degrades mRNAs after deadenylation (Decker and Parker 1993; Jacobs Anderson and Parker 1998; Tucker et al. 2001). Therefore, direct mRNA targets of the exonuclease activity should accumulate in the deadenylated form and not be identified by microarray analysis of poly(A)$^+$ RNA. Instead this analysis should reveal the physiological consequences of the *rrp44-exo*$^-$ mutation. The other mutation analyzed, *rrp44-endo*$^-$, changes Asp171 of the endonuclease active site to Ala and disrupts the endonuclease activity but has no significant effect on known RNA processing and degradation roles of the exosome (Lebreton et al. 2008; Schaeffer et al. 2009; Schneider et al. 2009).

In our analysis we focused on mRNAs that were up-regulated at least twofold in at least three of the four biological replicates. We were surprised that even though the *rrp44-exo*$^-$ mutation has a large effect on cell growth, the effects on gene expression were relatively modest, with 73 mRNAs up-regulated and 63 down-regulated (Table 1; Supplemental Table S1). We found no mRNAs that were affected by the *rrp44-endo*$^-$ mutation. Because the *rrp44-endo*$^-$ mutation has no measurable effect on growth or gene expression, it does not appear to perturb the cell even though the endoribonuclease active site is conserved in most if not all eukaryotes, and the activity has been shown to be conserved for the human ortholog hDIS3 (Tomecki et al. 2010). In addition to these mRNA targets, the *rrp44-exo*$^-$ microarray detected an increased level of polyadenylated ribosomal RNAs, which reflects the known role of the exosome in degradation of polyadenylated aberrant rRNAs (Kuai et al. 2004) and serves as a control to confirm the validity of the microarray approach.

We used gene ontology to analyze whether the mRNAs affected by the *rrp44-exo*$^-$ mutation were enriched in specific categories. All of the top gene ontology terms were related to iron uptake, including "iron chelate transport" ($P = 7 \times 10^{-11}$) and "iron ion homeostasis" ($P = 1 \times 10^{-9}$), and 16% of the mRNAs that were up-regulated were annotated with one or more gene ontology terms related to iron uptake (Table 1). To verify that the *rrp44-exo*$^-$ mutation indeed affected iron-starvation response genes, we isolated RNA from a second independently constructed *rrp44-exo*$^-$ mutant strain and analyzed it by Northern blotting with probes for the *FIT2* and *CTH2/TIS11* mRNAs. As shown in Figure 1A, expression of both genes was also induced in this *rrp44-exo*$^-$ strain. Therefore, we conclude that a major physiological consequence of the *rrp44-exo*$^-$ mutant is the up-regulation of the iron-starvation response.

The increased abundance of iron uptake-related mRNAs in an RNase mutant could be because that RNase directly degrades these mRNAs or because expression of a common regulator is affected by the RNase. The transcription factor Aft1 is a major contributor to the iron-starvation response and is known to bind to ANTGCACCC (Yamaguchi-Iwai et al. 1996; Zhu et al. 2009). We therefore searched the 6623 intergenic regions of the yeast genome for ANTGCACCC and found 59 occurrences in 52 different intergenic regions. These elements were highly enriched in the intergenic regions just upstream of genes affected by *rrp44-exo*$^-$. Specifically,

TABLE 1. Genes up at least twofold in three of four microarrays for *rrp44-exo*$^-$

Gene name	ORF	Fold up in rrp44-exo$^-$	Example iron-related GO-term	Perfect match for ANTGCACCC	Description
FIT2	YOR382W	7.7	Iron chelate transport	4	Siderophore-iron transporter
FIT3	YOR383C	5.5	Iron chelate transport		Siderophore-iron transporter
TIS11	YLR136C	5.5	Iron ion homeostasis	1	mRNA-binding protein expressed during iron starvation
ECM12	YHR021W-A	5.3			Nonessential protein of unknown function
PRM6	YML047C	5.1			Pheromone-regulated protein; predicted to have two transmembrane segments
SIT1	YEL065W	4.7	Iron chelate transport	1	Ferrioxamine B transporter
	YAL064W	4.1		1	Hypothetical protein
FIG1	YBR040W	4.0			Integral membrane; may participate in low affinity Ca^{2+} influx
AGA2	YGL032C	3.9			Adhesion subunit of a-agglutinin of a-cells
DIP5	YPL265W	3.9			Dicarboxylic amino acid permease
GRE1	YPL223C	3.9			Hydrophilin of unknown function; stress induced
ARN1	YHL040C	3.8	Iron chelate transport	1	Siderophore-iron transporter
HMX1	YLR205C	3.7	Iron ion homeostasis		Heme-binding peroxidase involved in the degradation of heme
NRD1	YNL251C	3.7			RNA-binding protein for 3′ end maturation of nonpolyadenylated RNAs
SET6	YPL165C	3.5			Protein of unknown function
ARP10	YDR106W	3.4			Actin-related protein
	YOL162W	3.4			Member of the Dal5p subfamily of the major facilitator family
PDH1	YPR002W	3.3			Mitochondrial protein that participates in respiration
GAT4	YIR013C	3.2			Protein containing GATA family zinc finger motifs
PRM5	YIL117C	3.2			Pheromone-regulated protein
HUG1	YML058W-A	3.2			Protein involved in the Mec1p-mediated checkpoint
VMR1	YHL035C	3.1		1	Member of the ATP-binding cassette (ABC) family; potential Cdc28p substrate
ARN2	YHL047C	3.1	Iron chelate transport	1	Siderophore-iron transporter
MAL33	YBR297W	3.1			MAL-activator protein
FRE2	YKL220C	3.1	Iron ion transport	1	Ferric reductase and cupric reductase
PRM2	YIL037C	3.0			Pheromone-regulated protein
TAD2	YJL035C	3.0			tRNA-specific adenosine-34 deaminase
IMD1	YAR073W	3.0			Nonfunctional protein with homology to IMP dehydrogenase
HES1	YOR237W	3.0			Regulation of ergosterol biosynthesis
TIR4	YOR009W	3.0			Cell wall mannoprotein
ALP1	YNL270C	2.9			Basic amino acid transporter
NCA3	YJL116C	2.9			Regulates expression of subunits 6 (Atp6p) and 8 (Atp8p) of the Fo-F1 ATP synthase
	YOL163W	2.9			Member of the Dal5p subfamily of the major facilitator family
COS12	YGL263W	2.9			Protein of unknown function
MIG2	YGL209W	2.9			Transcription factor involved in glucose repression
INO1	YJL153C	2.8			Inositol 1-phosphate synthase
CIN1	YOR349W	2.8			Tubulin folding factor
RKM5	YLR137W	2.8			Protein lysine methyltransferase
FUS2	YMR232W	2.7			Required for nuclear fusion during mating
FYV5	YCL058C	2.7			Involved in ion homeostasis
MND1	YGL183C	2.7			Protein required for recombination and meiotic nuclear division
MFA1	YDR461W	2.7			Mating pheromone a-factor

(continued)

TABLE 1. *Continued*

Gene name	ORF	Fold up in rrp44-exo$^-$	Example iron-related GO-term	Perfect match for ANTGCACCC	Description
	YLR108C	2.7			Hypothetical protein
AYT1	YLL063C	2.7			Acetyltransferase
ZPS1	YOL154W	2.7			GPI-anchored protein induced under low-zinc conditions
FLO1	YAR050W	2.7			Lectin-like protein involved in flocculation
FET3	YMR058W	2.6	Iron ion homeostasis		Ferro-O_2-oxidoreductase
ARG82	YDR173C	2.6			Transcription factor for Arg biosynthesis
	YNL024C	2.6			S-adenosylmethionine–dependent methyltransferase
PRM1	YNL279W	2.5			Protein involved in membrane fusion during mating
MIG3	YER028C	2.5			Transcriptional repressor involved in response to toxic agents such as hydroxyurea
ENB1	YOL158C	2.4	Iron chelate transport	2	Endosomal ferric enterobactin transporter
AAD14	YNL331C	2.4			Aryl-alcohol dehydrogenase
RRN3	YKL125W	2.4			Transcription of rDNA by RNA polymerase
SPS1	YDR523C	2.4			Protein serine/threonine kinase expressed at the end of meiosis
CCC2	YDR270W	2.4	Iron ion homeostasis	2	Cu^{2+}-transporting P-type ATPase
SNO1	YMR095C	2.4			Protein of unconfirmed function
	YIL089W	2.3			Hypothetical protein
DAN3	YBR301W	2.3			Cell wall mannoprotein
	YBR284W	2.3			Hypothetical protein
MTC3	YGL226W	2.3			Hypothetical protein
PCK1	YKR097W	2.3			Phosphoenolpyruvate carboxykinasein the cytosol
THI13	YDL244W	2.2			thiamine synthesis
LEE1	YPL054W	2.2			Zinc-finger protein of unknown function
CUE2	YKL090W	2.2			Protein of unknown function
FRE3	YOR381W	2.2	Iron chelate transport		Ferric reductase
ATG10	YLL042C	2.1			E2-like conjugating enzyme
HXT9	YJL219W	2.1			Putative hexose transporter
AIM4	YBR194W	2.1			Protein proposed to be associated with the nuclear pore complex
IDH1	YNL037C	2.1			Mitochondrial NAD(+)-dependent isocitrate dehydrogenase
SHU2	YDR078C	2.1			Protein of unassigned function involved in mutation suppression
KAR4	YCL055W	2.1			Transcription factor required for induction of KAR3 and CIK1 during mating
SRD1	YCR018C	2.0			Processing of pre-rRNA to mature rRNA

25% of the elements were found in the intergenic regions just upstream of the 73 genes in our data set, including four elements upstream of the most affected gene (*FIT2*) (Table 1). Several other genes that were affected by *rrp44-exo*$^-$ had ANTGCACCC elements nearby or had imperfect matches. In addition, several genes that were induced less than our two-fold threshold also had ANTGCACCC elements. We thus suspected that the *rrp44-exo*$^-$ mutation somehow affected the activity of the transcription factor Aft1, which in turn increased transcription of iron-uptake–related genes.

To test whether Aft1 activity is increased in the *rrp44-exo*$^-$ mutant, we constructed a *lacZ* reporter gene by cloning the binding site for Aft1 into a construct that contained a minimal promoter and the *lacZ* ORF. The resulting reporter plasmid was transformed into *rrp44-exo*$^-$ and *RRP44* strains, and β-galactosidase activity was measured in three transformants for each strain. Figure 1B shows that β-galactosidase levels were increased 2.3-fold in the *rrp44-exo*$^-$ strain, which matches the effect we see on iron-starvation regulon genes. Expression of β-galactosidase from the parental plasmid that lacks an Aft1 binding site was not affected (Fig. 1B; Supplemental Fig. 1). These data suggest that the Aft1 transcription factor is indeed more active in the *rrp44-exo*$^-$ mutant.

Aft1 regulation is mostly post-translational, such that Aft1 is localized in the cytoplasm under iron replete conditions and becomes relocalized to the nucleus when the cell senses a need for more iron (Yamaguchi-Iwai et al. 2002). We therefore compared the location of an Aft1-GFP fusion protein in

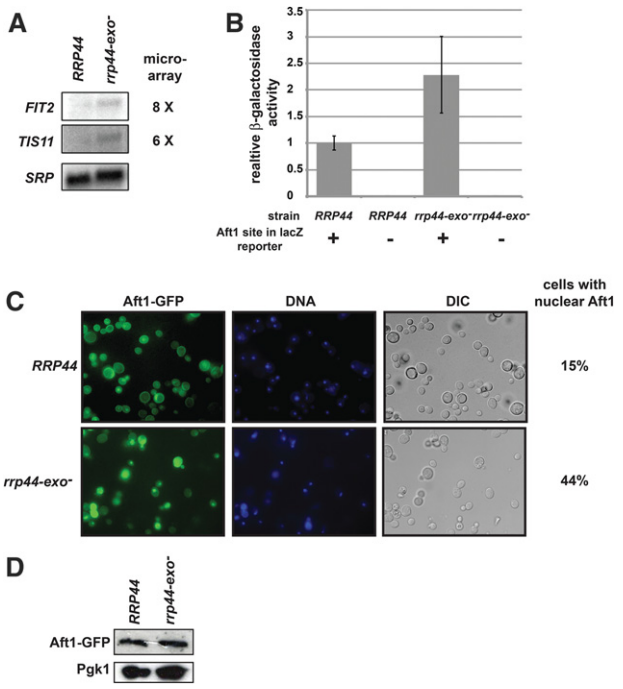

FIGURE 1. The Aft1 regulated iron regulon is activated in a *rrp44-exo*$^-$ mutant. (*A*) Northern blot analysis confirms the microarray results that the expression of *FIT2* and *TIS11* mRNAs is increased in an *rrp44-exo*$^-$ mutant. To the *left* of the blot is the fold increase in expression from the microarray analysis. SRP indicates the RNA subunit of the signal recognition particle, which is used as a loading control. (*B*) The *rrp44-exo*$^-$ mutation increases expression of a *lacZ* reporter gene that contains a single Aft1 binding site. The graph shows averages and standard deviations of triplicate cultures. As a control, a reporter gene without an Aft1 binding site is very poorly expressed and not affected by *rrp44-exo*$^-$ (see Supplemental Fig. 1). (*C*) An Aft1-GFP fusion protein was expressed in wild-type and *rrp44-exo*$^-$ mutant strains to localize Aft1. The percentage of cells that showed a nuclear localization of Aft1, reflecting activation of Aft1, is indicated on the *right*. (*D*) Western blot analysis of Aft1-GFP in wild-type and *rrp44-exo*$^-$ strains, using anti-GFP antibody. Pgk1 is used for loading control.

the *rrp44-exo*$^-$ mutant and *RRP44* strains. Aft1 was observed to be concentrated in the nucleus of 44% of the *rrp44-exo*$^-$ cells and in 15% of the *RRP44* cells (Fig. 1C). We also analyzed expression levels of Aft1-GFP by Western blot and noted that they were similar in the wild-type and *rrp44-exo*$^-$ strains (Fig. 1D). The enrichment of ANTGCACCC elements, increase in *lacZ* expression, and increased nuclear localization of Aft1 all indicate that the *rrp44-exo*$^-$ mutant activates the cellular iron-starvation response by somehow activating and relocalizing this key transcription factor.

Inactivation of the exonuclease activity of Rrp44 increases hydrogen peroxide sensitivity and intracellular ROS levels

Iron is both an essential element because it is a cofactor for many proteins and a toxic element because iron reacts to generate ROS. To further characterize the effect of the increase in Aft1 activity and the resulting up-regulation of the iron-starvation regulon, we analyzed growth under low- and high-iron conditions, as well as oxidative stress. To analyze the effect of iron concentration in the media, we compared four different growth conditions: SC media with the standard iron concentration (0.2 mg/L $FeCl_3$), SC media with 1000-fold increase in iron, SC media with no added iron but with trace iron available from the water or other ingredients, and SC media with no added iron and added iron chelator bathophenanthrolinedisulfonate (BPS). These conditions did not reveal any specific effects on the *rrp44-exo*$^-$ mutant; the *rrp44-exo*$^-$ mutant grows slower than an isogenic *RRP44* strain under the first three conditions, and neither the wild-type nor mutant strains grew in the presence of BPS. We conclude that the up-regulation of the iron-starvation regulon we detected in the *rrp44-exo*$^-$ strain does not significantly affect its ability to grow under iron-excess or iron-starvation conditions.

To test the effects of *rrp44-exo*$^-$ mutant further, we tested if this mutant was sensitive to exposure to oxidative stress. As shown in Figure 2A, the *rrp44-exo*$^-$ mutant did not grow on

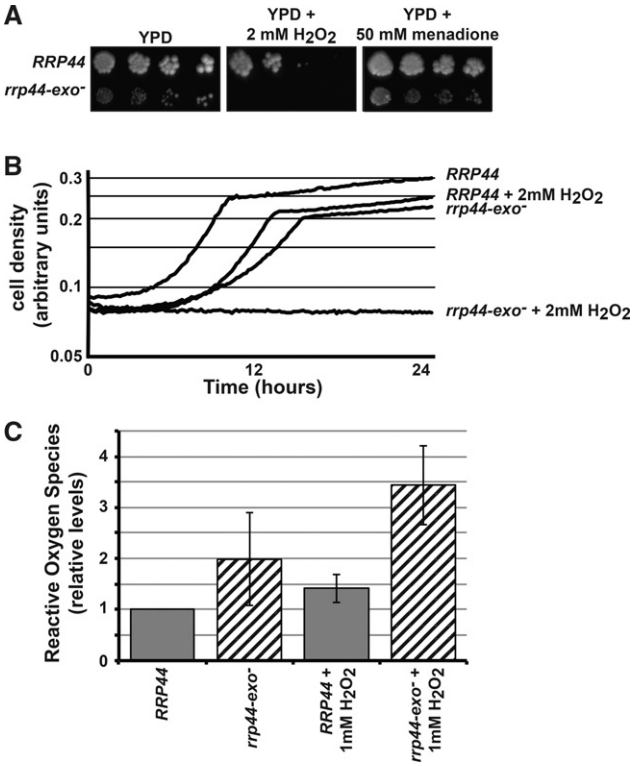

FIGURE 2. The *rrp44-exo*$^-$ is hypersensitive to H_2O_2. (*A*) The *rrp44-exo*$^-$ mutant is hypersensitive to hydrogen peroxide when grown on solid media. Shown are the *RRP44* and *rrp44-exo*$^-$ strains grown on solid media either without added reactive oxygen species (ROS) or with added hydrogen peroxide or the superoxide generating compound menadione. (*B*) Shown are growth curves of the *RRP44* and *rrp44-exo*$^-$ strains grown in liquid media in the presence or absence of H_2O_2. (*C*) The *rrp44-exo*$^-$ strain hyperaccumulates ROS. Intracellular ROS levels were measured in *RRP44* and *rrp44-exo*$^-$ strains grown in the presence or absence of 1 mM H_2O_2.

YPD plates supplemented with 2 mM H_2O_2, indicating increased sensitivity to oxidative stress. Under these same conditions, the wild-type strain did grow, although at a slightly slower rate than in the absence of H_2O_2. We observed similar effects during growth in liquid media: Addition of 2 mM H_2O_2 had a modest effect on the growth rate of the *RRP44* control strain but completely eliminated growth of the *rrp44-exo*$^-$ mutant (Fig. 2B). This hypersensitivity was specific to H_2O_2 because the superoxide-generating agent menadione affected the wild type and the *rrp44-exo*$^-$ mutant approximately equally (Fig. 2A). In addition to the low- and high-iron stress. other stresses such as growth at high or low temperature did not specifically affect the growth of the *rrp44-exo*$^-$ strain compared with the wild type, further demonstrating the specificity of the H_2O_2 sensitivity.

Hypersensitivity to oxidative stress could result from inability to repair damage caused by normal levels of ROS, it could be due to increased levels of intracellular ROS, or both. To test whether ROS levels were altered in the *rrp44-exo*$^-$ mutant, we used 2′,7′-dichlorodihydrofluorescein diacetate (H_2DCFDA). H_2DCFDA is not fluorescent, but upon hydrolysis by intracellular esterases and oxidation by ROS, it is transformed into the fluorescent compound 2′,7′-dichlorofluorescein (DCF). Thus, intracellular ROS levels can be detected by measuring fluorescence after H_2DCFDA exposure. By use of this assay, we detected a 2.0-fold higher level of ROS in the *rrp44-exo*$^-$ mutant compared with the mutant during growth in the absence of added ROS and a 2.4-fold higher level after exposure to 1 mM H_2O_2 (Fig. 2C). We therefore conclude that the *rrp44-exo*$^-$ mutant accumulates increased amounts of ROS.

Altered iron response and sensitivity to oxidative stress in the *rrp44-exo*$^-$ mutant are functionally connected

Knowing the *rrp44-exo*$^-$ mutant has both an up-regulated iron response and increased ROS, we decided to test if these were related. We could envision at least two possible ways these are linked. Aft1 activity is not directly controlled by iron but instead is controlled by the availability of iron-sulfur clusters (Chen et al. 2004; Rutherford et al. 2005). Since hydrogen peroxide damages iron-sulfur clusters, it is possible that the excess ROS in *rrp44-exo*$^-$ decreases the availability of iron-sulfur clusters, which would result in Aft1 induction. Thus, under this scenario the *rrp44-exo*$^-$ mutant responds appropriately to a decreased level of available iron-sulfur clusters that is caused by an increased ROS level. Alternatively, *rrp44-exo*$^-$ may inappropriately up-regulate Aft1 and the resulting increased intracellular Fe levels would cause an increased production of ROS due to the reactivity of iron ions.

To distinguish between these two possibilities, we first exposed the *rrp44-exo*$^-$ mutant to 1 mM H_2O_2 for 1 h and then removed the H_2O_2 and added extra iron to the media. This addition of extra iron after H_2O_2 exposure increased growth of the *rrp44-exo*$^-$ strain. (Fig. 3A, cf. red and green solid lines). In comparison, adding iron to *RRP44* cells that were treated with ROS did not significantly change their growth (Fig. 3A, dashed lines). Similarly, adding iron to *rrp44-exo*$^-$ or *RRP44* in the absence of H_2O_2 stress did not significantly affect their growth (Fig. 3B). These data support the first possibility that increased ROS levels lead to a decreased level of available iron-sulfur clusters, which in turn results in Aft1 activation. This possibility suggests that adding H_2O_2 to *RRP44* cells should have a similar effect of Aft1 activation. Figure 3C shows that, indeed, the *FIT2* mRNA is up-regulated upon exposure of wild-type cells to H_2O_2. The effects of H_2O_2 and *rrp44-exo*$^-$ were not additive; at low concentrations of H_2O_2, the *rrp44-exo*$^-$ mutant did not show a further increase in *FIT2* expression, while at higher concentrations of H_2O_2, the *RRP44* and *rrp44-exo*$^-$ strains responded similarly (Fig. 3C). Taken together, these data suggest that the *rrp44-exo*$^-$ mutant has a higher requirement for iron and responds appropriately to this requirement by up-regulating the iron regulon.

The exonuclease activity of the exosome is required for normal growth rate during fermentative conditions but not during respiratory conditions

When yeast is grown under standard laboratory conditions in YEP + 2% glucose, it initially ferments the glucose to ethanol and, only after glucose is depleted, respires the ethanol to CO_2. The above experiments and most published experiments with exosome mutants use log phase cells that almost exclusively ferment. Under these circumstances, ROS production is relatively low, and iron needs are likely to be low as well, since a number of mitochondrial proteins required for respiration contain Fe-S clusters. Therefore, to extend our understanding of the physiological effects of the *rrp44-exo*$^-$ mutant beyond the fermentative conditions, we compared its growth rate to the wild-type strain under conditions where yeast can only respire. Specifically, we compared growth rates of wild-type cells and the *rrp44-exo*$^-$ mutant on media with glycerol or ethanol instead of glucose as a carbon source. Glycerol and ethanol are nonfermentable and require the cells to grow by respiration. Figure 4A shows that wild-type and *rrp44-exo*$^-$ strains grow with similar rates when grown on YEP plates with 2% glycerol or 2% ethanol. Growth in liquid culture revealed that the *rrp44-exo*$^-$ mutant grew slightly slower than the wild type, but the difference was much less pronounced than during fermentative growth (Fig. 4B). To test whether expression of Rrp44 was different during fermentative and respiratory growth, we performed Western blot on an epitope-tagged strain. Figure 4C shows that Rrp44 levels during growth on YPD and YEP + 2% glycerol were similar. Thus, the less-pronounced growth defect of *Rrp44-exo*$^-$ during respiratory growth is not correlated with reduced expression of the protein.

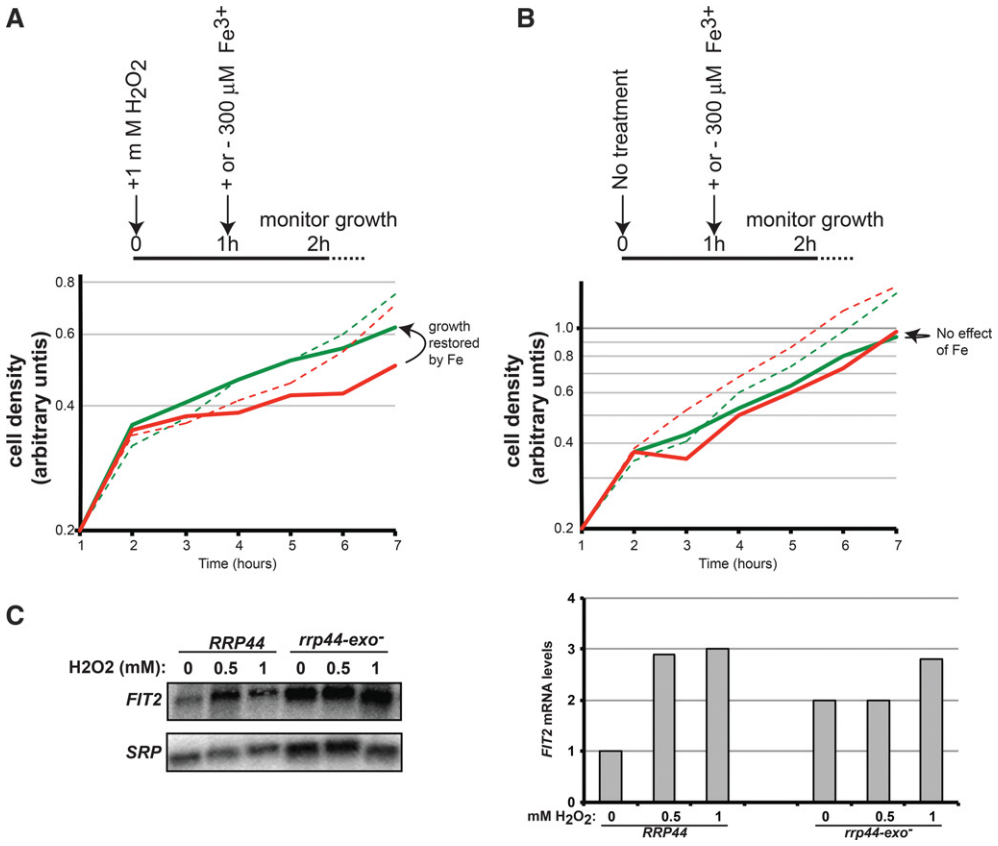

FIGURE 3. Sensitivity to oxidative stress in the *rrp44-exo*$^-$ mutant is functionally related to the altered iron response. (*A*) Growth inhibition of the *rrp44-exo*$^-$ after 1 h exposure to 1 mM H_2O_2 can be suppressed by addition of extra iron to the media. Solid lines indicate growth curves of the *rrp44-exo*$^-$ mutant; dashed lines, growth curves of a *RRP44* control strain. Green indicates growth after addition of iron; red, growth in the absence of extra iron. (*B*) Addition of extra iron has no effect in the absence of prior H_2O_2 treatment. Colors and solid versus dashed lines as in *A*. (*C*) The *FIT2* mRNA is induced by exposure to H_2O_2, and this effect is not additive with the effect of the *rrp44-exo*$^-$ mutation. Shown is a representative Northern blot (*left*) and its quantitation (*right*). The SRP RNA served as a loading control as in Figure 1.

Our observations that the *rrp44-exo*$^-$ strain is hypersensitive to ROS and has a slow growth phenotype specifically during fermentative growth appear paradoxical, since ROS production should be low during fermentation. To resolve this puzzle, we measured ROS levels during respiratory growth and found that under these conditions the *rrp44-exo*$^-$ mutant had levels of ROS comparable to wild type (Fig. 4C), presumably because mechanisms to detoxify ROS are also up-regulated during respiratory growth. Thus, these observations further strengthen the correlation between the growth defect of *rrp44-exo*$^-$ and ROS accumulation.

Because the *rrp44-exo*$^-$ mutant has a growth defect during fermentative growth on glucose but has much less of a growth defect during respiratory growth, we also analyzed whether it was inefficient in converting glucose to biomass. Specifically, we simultaneously measured biomass accumulation (by measuring optical density) and glucose depletion during growth in YEP + 2% glucose. As shown in Figure 4D the wild type and *rrp44-exo*$^-$ mutant converted glucose to biomass with very similar efficiency. Therefore, the slow growth during fermentation is not due to inefficient conversion of glucose to biomass.

The exonuclease activity of the exosome is required for RNA processing and degradation during fermentative and respiratory conditions

Yeast growth is typically coordinated with ribosome production (Waldron and Lacroute 1975; Mager and Planta 1991). This suggests the possibility that the slow growth phenotype of the *rrp44-exo*$^-$ strain is related to its known defect in ribosomal RNA maturation. Thus, to characterize the relation between slow growth and this rRNA processing defect, we isolated RNA from the wild-type and *rrp44-exo*$^-$ mutant strains growing in fermentative or respiratory conditions and analyzed it by Northern blotting. Figure 5A shows that the aberrant 5.8S rRNA processing intermediates present in the *rrp44-exo*$^-$ strain during growth on glucose are also present during growth on glycerol (marked with an asterisk in Fig. 5). Similarly, the known defects of the *rrp44-exo*$^-$ mutant in 5′ ETS degradation (Fig. 5B) and U4 snRNA (Fig. 5C) processing were present, even when grown on glycerol. Therefore, we conclude that the growth defect exhibited by *rrp44-exo*$^-$ during fermentative growth is independent of these specific processing and degradation defects and that

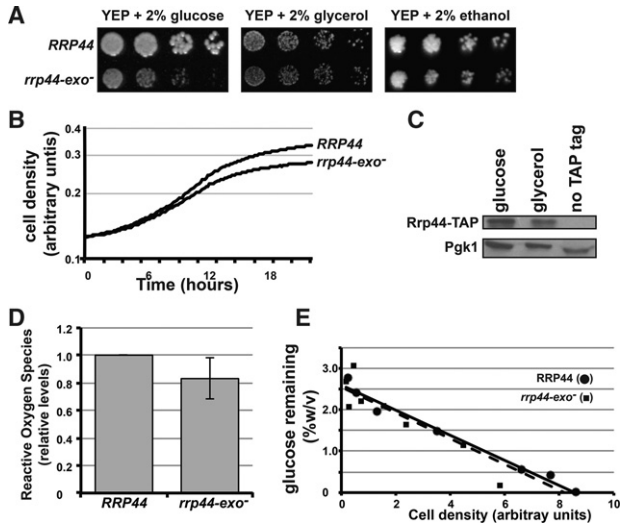

FIGURE 4. Lack of the Rrp44 exonuclease activity results in slow growth under fermentative but not respiratory growth. (*A*) Shown are the *RRP44* and *rrp44-exo*$^-$ strains grown on solid media either with fermentable glucose or with nonfermentable glycerol or ethanol as the carbon source. (*B*) Shown are growth curves of the *RRP44* and *rrp44-exo*$^-$ strains grown in liquid media with glycerol as the carbon source (cf. with the growth in medium with glucose in Fig. 2A). (*C*) Western blot analysis of TAP-tagged Rrp44 levels during fermentative (glucose) and respiratory (glycerol) growth. Pgk1 is used as a loading control. (*D*) The *rrp44-exo*$^-$ strain does not hyperaccumulate intracellular ROS when grown in media with glycerol as the carbon source (cf. with ROS accumulation when grown in media with glucose in Fig. 2C). (*E*) The *rrp44-exo*$^-$ mutant grows slowly in media containing glucose but is not inefficient in converting glucose to biomass. The mutant and wild-type strains were grown in YPD media, and growth (OD_{600}) and glucose levels were monitored every 2 h and plotted.

the exonuclease activity of the exosome is required for RNA processing and degradation during fermentative and respiratory conditions.

CONCLUSIONS

Our results suggest that the major physiological consequence of inactivating the exonuclease of Rrp44 is an increase in ROS accumulation, which results in an increased need for iron and a decreased growth rate under fermentative conditions. Although the RNA exosome has been extensively studied at the molecular level and mutants that reduce RNA exosome activity cause slow growth, how the RNA exosome affects the physiological state of the cell was previously largely unknown. To investigate this, we used a microarray approach to identify genes that were up- or down-regulated in response to inactivating the active site residues of the main catalytic subunit of the exosome. Despite the very slow growth of the *rrp44-exo*$^-$ strain, the number of genes affected was surprisingly low and dominated by genes in the iron-uptake regulon. The main transcription factor for this regulon is Aft1, and we show that expression of a *lacZ* reporter gene that incorporates a single binding site for Aft1 is increased in the *rrp44-exo*$^-$ mutant. We further confirmed that Aft1 is activated by showing that a GFP fusion is translocated into the nucleus. Aft1 activation and nuclear import have been shown to be directed by a pair of glutaredoxins (Grx3 and Grx4), which by an unknown mechanism respond to the level of available iron-sulfur clusters (Ojeda et al. 2006; Pujol-Carrion et al. 2006).

Strikingly, three different RNases and RNA degradation pathways have previously been implicated in the regulation of the iron response. First, *RRP6* encodes a nuclear cofactor of the exosome, and iron regulon RNAs were shown to increase in *rrp6Δ* strains (Lee et al. 2005; Houalla et al. 2006; Ciais et al. 2008). The molecular mechanism behind this up-regulation was not fully explored, but it was suggested that iron regulon mRNAs were likely direct targets of the nuclear exosome (Lee et al. 2005; Houalla et al. 2006; Ciais et al. 2008). In contrast, our findings of up-regulation in *rrp44-exo*$^-$ can be fully explained by activation of the Aft1 transcription factor, and we do not suspect that these mRNAs are direct Rrp44 targets. A further difference is that the increased *CTH2* mRNA level in *rrp6Δ* is mostly due to accumulation of 3′ extended mRNAs (Ciais et al. 2008), which we did not detect in *rrp44-exo*$^-$. Thus *rrp6Δ* and *rrp44-exo*$^-$ appear to have different effects on iron regulon mRNAs, which likely reflect two different mechanisms of control. The second RNase previously implicated in expression of iron-uptake–related mRNAs is the endonuclease Rnt1 (Lee et al. 2005). Rnt1 and Rrp44 also appear to function in separate pathways because genes up-regulated in *rnt1Δ* were not enriched for Aft1 targets, *rnt1Δ* resulted in decreased expression of lacZ reporter under Aft1 control while *rrp44-exo*$^-$ resulted in an increased expression, and the *rrp44-exo*$^-$ mutation increases expression of *FIT2* mRNA while *rnt1Δ* decreases its expression. Finally, CTH2, one of the Aft1 targets that we find up-regulated in *rrp44-exo*$^-$, encodes an RNA binding protein that controls decapping of specific mRNAs by Dcp2 followed by Xrn1-mediated degradation (Puig et al. 2005; Pedro-Segura et al. 2008), but the target mRNAs of Cth2 differ from the Aft1 targets that we find up-regulated in *rrp44-exo*$^-$. Recently, a second RNA binding protein, Air2, has also been implicated in the regulation of the iron regulon (Schmidt et al. 2012). Air2 is a cofactor of the exosome and Schmidt et al. (2012) reported that the *FIT2* mRNA level is reduced in an *rrp6Δ* strain but increased in an *rrp6Δ air2Δ* double mutant. This suggests that Air2p acts in an Rrp6-independent pathway to affect *FIT2* mRNA. Whether this Air2-dependent pathway is the same as the pathway we describe here remains to be determined. Overall, these results indicate that iron homeostasis is regulated by at least four different RNases—Rrp44, Rrp6, Rnt1, and Dcp2/Xrn1, and the available evidence indicates that each of these RNases acts in different pathways.

We also show that the *rrp44-exo*$^-$ mutant strain accumulates ROS. Because ROS are especially reactive with iron-sulfur clusters, we hypothesize that this increased ROS causes a

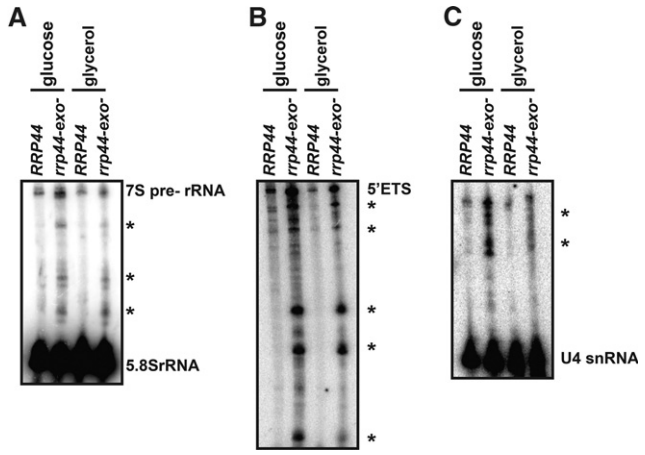

FIGURE 5. Although the growth defect of *rrp44-exo*$^-$ is specific for fermentative growth, the known RNA processing defects are seen during both fermentative and respiratory growth. The *RRP44* and *rrp44-exo*$^-$ strains were grown in YEP + glucose or YEP + glycerol as indicated. RNA was isolated and analyzed by Northern blotting with probes specific for 5.8S rRNA (*A*), the 5′ external transcribed spacer of the pre-rRNA (5′ ETS; *B*), or the U4 snRNA (*C*). RNA species that accumulate in the *rrp44-exo*$^-$ mutant are indicated with asterisks.

reduction in the level of iron-sulfur clusters, which turns on the Aft1 regulon. Our observations that the hydrogen peroxide sensitivity of *rrp44-exo*$^-$ can be suppressed by adding iron and that the iron regulon is induced upon addition of hydrogen peroxide to wild-type cells are consistent with this possibility. The molecular mechanism of how the exonuclease activity of the RNA exosome affects this signaling pathway remains unknown. However, the exosome has been shown to be required for the degradation of long noncoding RNAs (Lebreton et al. 2008), which can affect gene expression. For example, the expression of *SER3* in response to serine starvation is regulated by the noncoding RNA SRG1 (Martens et al. 2004, 2005). One possibility is that a similar noncoding RNA affects expression of a key regulator that controls ROS levels.

Although the exosome has many known functions, it is not known which of these functions is most critical for normal growth or whether multiple important aspects of cell physiology are perturbed in exosome mutants. Here we show that the growth defect of *rrp44-exo*$^-$ is much more severe under fermentative conditions than under respiratory conditions. In addition, under conditions where *rrp44-exo*$^-$ grows slowly, this strain hyperaccumulates ROS, whereas under conditions where it does not hyperaccumulate ROS, growth is much more similar to that of the wild type. In contrast, the 5.8S rRNA and U4snRNA processing and 5′ ETS degradation defects seen in the mutant do not correlate with a defect in growth rate. Thus, our results suggest the possibility that the ROS hyperaccumulation we observe is a major contributor to the slow growth seen in this and possibly other exosome mutants.

MATERIALS AND METHODS

Yeast strains

All strains were derived from the heterozygous diploid *RRP44/rrp44Δ::NEO* strain obtained from Open Biosystems using standard yeast genetics techniques as previously described (Schaeffer et al. 2009). The microarray analysis was done on quadruplicate cultures of yAV1129, yAV1131, and yAV1135. Follow-up experiments were done with these same strains as well as a second independent isolate of *rrp44-exo*$^-$, yAV1284. All experiments were done at least in duplicate. To generate a second independent isolate of *rrp44-exo*$^-$, first the ORF for NEO resistance was replaced by an ORF encoding Nourseothricin resistance (NAT) by transforming the *RRP44/rrp44Δ::NEO* strain obtained from Open Biosystems with p4339 (Tong and Boone 2006) obtained from Dr. Charlie Boone's laboratory. Next the *rrp44-exo*$^-$ plasmid was introduced as previously described (Schaeffer et al. 2009). The genotypes of the strains used are as follows:

yAV1129 (wild-type strain): *Mat*α, *leu2-Δ0*, *ura3-Δ0*, *his3-Δ1*, *rrp44Δ*::NEO [RRP44, LEU2];
yAV1131 (*rrp44-exo*$^-$): *Mat*α, *leu2-Δ0*, *ura3-Δ0*, *his3-Δ1*, *rrp44Δ*::NEO [*rrp44D551N*, LEU2];
yAV1135 (*rrp44-endo*$^-$): *Mat*α, *leu2-Δ0*, *ura3-Δ0*, *his3-Δ1*, *rrp44Δ*::NEO [*rrp44D171A*, LEU2]; and
yAV1284 (*rrp44-exo*$^-$): *leu2-Δ0*, *ura3-Δ0*, *his3-Δ1*, *lys2-Δ0*, *rrp44Δ*::*NAT* [*rrp44D551N*, LEU2].

Plasmids

The *RRP44*, *rrp44-exo*$^-$, and *rrp44-endo*$^-$ plasmids have previously been described (Schaeffer et al. 2009). The Aft1-GFP plasmid has also been described (Crisp et al. 2003) and was kindly provided by Dr. Jerry Kaplan (University of Utah). The *lacZ* control plasmid pCM64 was kindly provided by Dr. Kevin Morano (University of Texas Health Science Center Houston). pCM64 is a derivative of pLG669-Z (Guarente and Ptashne 1981) with the 434-bp XhoI fragment replaced with a linker introducing a unique BglII site. The Aft1-*lacZ* reporter plasmid pAV804 is a derivative of PCM64 with the Aft1 binding site form the FET3 promoter inserted into the unique BglII site. pAV804 was generated by cloning oAV886 (GATCTCTTCAAAAGTGCACCCATTTGCAGGTGCTCC) and oAV887 (TCGAGGAGCACCTGCAAATGGGTGCACTTTTGAAGA) into the BglII site of pCM64.

Media and growth conditions

All growth assays were repeated at least three times. Unless otherwise indicated, all cultures were started overnight in 5 mL YPD and then transferred the following day to the specified media. Growth was at 30°C unless otherwise noted. YPD (YEP + glucose), YEP + glycerol, YEP + ethanol, and SC media were prepared as previously described (Burke et al. 2000). Yeast nitrogen base (catalog no. 1501-250), yeast nitrogen base lacking iron (catalog no. 1551-100), and the amino acids mixes were from Sunrise Science. The iron chelator BPS was from Sigma-Aldrich (catalog no. 146617-1G). For the experiments in Figure 3, ammonium iron(III) sulfate dodecahydrate was from Sigma Aldrich (catalog no. 221260-25G). Glucose levels were

measured using a glucose (HK) assay kit (Sigma-Aldrich catalog no. GAHK20-1KT) according to the manufacturer's instructions.

For growth assays on solid media, fivefold serial dilutions of *S. cerevisiae* cells were made in a 96-well plate starting with $OD_{600} = 0.6$. These were then spotted on the indicated media and incubated at 30°C (unless otherwise indicated).

Liquid growth assays were performed either in 96-well plates in a Synergy MX automated microplate reader or in test tubes.

Microscopy

Cells were transformed with the Aft1-GFP plasmid and grown in selective media. Before microscopy, cells were stained with Hoechst 33342 stain for 10 min, washed with H_2O, and observed with an Olympus IX81 microscope.

β-galactosidase assay

Strains containing either pCM64 or pAV804 were grown to $OD_{600} = 0.6$, and β-galactosidase activity was measured using the Beta-Glo reagent (Promega) according to the manufacturer's instructions using a Biotech Synergy MX plate reader. Briefly, 50 µL of culture was mixed with 50 µL of β-glo reagent in a 96-well microtiter plate, incubated for 30 min, and light production measured and normalized to OD_{600}. Similar results were obtained when β-galactosidase activity was measured using ortho-nitrophenyl-β-galactoside (ONPG).

ROS detection

Cultures were either treated with the indicated concentrations of H_2O_2 or left untreated. After 1 h treatment, 1 mL of culture was centrifuged and the cells washed in phosphate buffered saline (PBS) and resuspended in 1 mL PBS containing 25 µM H2DCFDA. Fluorescence was detected at 525 nm with excitation at 495 nm. Fluorescence was normalized to OD_{600}.

RNA isolation and analysis

Liquid cultures (5 mL) were grown overnight at 30°C. The cultures were then diluted into 20 mL of fresh media to an OD_{600} of 0.125 and grown at 30°C to an OD_{600} of 0.6. The culture was briefly centrifuged, and the cell pellet was collected, washed once with ddH_2O, and either used immediately or frozen at −80°C prior to RNA extraction. RNA was extracted as previously described (He et al. 2008), separated on 6% polyacrylamide or 1.3% agarose gels, and blotted onto Zeta-Probe membrane (Biorad). The blots were probed with $5'P^{32}$-labeled oligonucleotides for *FIT2* mRNA (CGACGG CTTGAGTGACGGTC), *TIS11* mRNA (GGGAGTTTCCTGCAC TTGGC), 5.8S rRNA (TTTCGCTGCGTTCTTCATC), 5′ ETS (CGAACGACAAGCCTACTG), U4 snRNA (CGGACGAATCCT CACTGATA), and the RNA subunit of the signal recognition particle (SRP; GTCTAGCCGCGAGGAAGG) as a loading control.

For the microarray experiments, quadruplicate cultures of yAV1129, yAV1131, and yAV1135 were grown in YPD, and RNA was isolated and processed as described previously (He et al. 2003). Fragmented cRNA was prepared using the Affymetrix 3′IVT express kit and was hybridized to Affymetrix Yeast Genome 2.0 arrays. The relative abundance of each transcript was determined using Affymetrix Microarray Suite 5.0.

SUPPLEMENTAL MATERIAL

Supplemental material is available for this article.

ACKNOWLEDGMENTS

We thank Drs. Kevin Morano, Charlie Boone, and Jerry Kaplan for plasmids, as well as Kevin Morano for use of the 96-well plate reader. This work was supported by grants from the NIH (5R01GM099790) and The Welch Foundation (AU-1773) to A.v.H. and from the NIH (R37GM27757) to A.J.

Received October 30, 2013; accepted April 1, 2014.

REFERENCES

Allmang C, Kufel J, Chanfreau G, Mitchell P, Petfalski E, Tollervey D. 1999a. Functions of the exosome in rRNA, snoRNA and snRNA synthesis. *EMBO J* **18:** 5399–5410.

Allmang C, Petfalski E, Podtelejnikov A, Mann M, Tollervey D, Mitchell P. 1999b. The yeast exosome and human PM–Scl are related complexes of 3′→5′ exonucleases. *Genes Dev* **13:** 2148–2158.

Brieger K, Schiavone S, Miller FJ Jr, Krause KH. 2012. Reactive oxygen species: from health to disease. *Swiss Med Wkly* **142:** w13659.

Burke D, Dawson D, Stearns T. 2000. *Methods in yeast genetics: a Cold Spring Harbor Laboratory course manual*. Cold Spring Harbor Laboratory Press, Cold Spring Harbor, NY.

Chekanova JA, Dutko JA, Mian IS, Belostotsky DA. 2002. *Arabidopsis thaliana* exosome subunit AtRrp4p is a hydrolytic 3′→5′ exonuclease containing S1 and KH RNA-binding domains. *Nucleic Acids Res* **30:** 695–700.

Chekanova JA, Gregory BD, Reverdatto SV, Chen H, Kumar R, Hooker T, Yazaki J, Li P, Skiba N, Peng Q, et al. 2007. Genome-wide high-resolution mapping of exosome substrates reveals hidden features in the *Arabidopsis* transcriptome. *Cell* **131:** 1340–1353.

Chen K, Keaney JF Jr. 2012. Evolving concepts of oxidative stress and reactive oxygen species in cardiovascular disease. *Curr Atheroscler Rep* **14:** 476–483.

Chen OS, Crisp RJ, Valachovic M, Bard M, Winge DR, Kaplan J. 2004. Transcription of the yeast iron regulon does not respond directly to iron but rather to iron-sulfur cluster biosynthesis. *J Biol Chem* **279:** 29513–29518.

Ciais D, Bohnsack MT, Tollervey D. 2008. The mRNA encoding the yeast ARE-binding protein Cth2 is generated by a novel 3′ processing pathway. *Nucleic Acids Res* **36:** 3075–3084.

Crisp RJ, Pollington A, Galea C, Jaron S, Yamaguchi-Iwai Y, Kaplan J. 2003. Inhibition of heme biosynthesis prevents transcription of iron uptake genes in yeast. *J Biol Chem* **278:** 45499–45506.

Decker CJ, Parker R. 1993. A turnover pathway for both stable and unstable mRNAs in yeast: evidence for a requirement for deadenylation. *Genes Dev* **7:** 1632–1643.

Dziembowski A, Lorentzen E, Conti E, Seraphin B. 2007. A single subunit, Dis3, is essentially responsible for yeast exosome core activity. *Nat Struct Mol Biol* **14:** 15–22.

Evguenieva-Hackenberg E, Walter P, Hochleitner E, Lottspeich F, Klug G. 2003. An exosome-like complex in *Sulfolobus solfataricus*. *EMBO Rep* **4:** 889–893.

Gomez-Cabrera MC, Sanchis-Gomar F, Garcia-Valles R, Pareja-Galeano H, Gambini J, Borras C, Vina J. 2012. Mitochondria as sources and targets of damage in cellular aging. *Clin Chem Lab Med* **50:** 1287–1295.

Guarente L, Ptashne M. 1981. Fusion of *Escherichia coli lacZ* to the cytochrome *c* gene of *Saccharomyces cerevisiae*. *Proc Natl Acad Sci* **78:** 2199–2203.

Guo J, Cheng P, Yuan H, Liu Y. 2009. The exosome regulates circadian gene expression in a posttranscriptional negative feedback loop. *Cell* **138:** 1236–1246.

He F, Li X, Spatrick P, Casillo R, Dong S, Jacobson A. 2003. Genome-wide analysis of mRNAs regulated by the nonsense-mediated and 5′ to 3′ mRNA decay pathways in yeast. *Mol Cell* **12:** 1439–1452.

He F, Amrani N, Johansson MJ, Jacobson A. 2008. Chapter 6. Qualitative and quantitative assessment of the activity of the yeast nonsense-mediated mRNA decay pathway. *Methods Enzymol* **449:** 127–147.

Herrero E, Ros J, Belli G, Cabiscol E. 2008. Redox control and oxidative stress in yeast cells. *Biochim Biophys Acta* **1780:** 1217–1235.

Houalla R, Devaux F, Fatica A, Kufel J, Barrass D, Torchet C, Tollervey D. 2006. Microarray detection of novel nuclear RNA substrates for the exosome. *Yeast* **23:** 439–454.

Jacobs Anderson JS, Parker RP. 1998. The 3′ to 5′ degradation of yeast mRNAs is a general mechanism for mRNA turnover that requires the SKI2 DEVH box protein and 3′ to 5′ exonucleases of the exosome complex. *EMBO J* **17:** 1497–1506.

Kadaba S, Krueger A, Trice T, Krecic AM, Hinnebusch AG, Anderson J. 2004. Nuclear surveillance and degradation of hypomodified initiator $tRNA^{Met}$ in *S. cerevisiae*. *Genes Dev* **18:** 1227–1240.

Kuai L, Fang F, Butler JS, Sherman F. 2004. Polyadenylation of rRNA in *Saccharomyces cerevisiae*. *Proc Natl Acad Sci* **101:** 8581–8586.

Lebreton A, Tomecki R, Dziembowski A, Seraphin B. 2008. Endonucleolytic RNA cleavage by a eukaryotic exosome. *Nature* **456:** 993–996.

Lee A, Henras AK, Chanfreau G. 2005. Multiple RNA surveillance pathways limit aberrant expression of iron uptake mRNAs and prevent iron toxicity in *S. cerevisiae*. *Mol Cell* **19:** 39–51.

Mager WH, Planta RJ. 1991. Coordinate expression of ribosomal protein genes in yeast as a function of cellular growth rate. *Mol Cell Biochem* **104:** 181–187.

Martens JA, Laprade L, Winston F. 2004. Intergenic transcription is required to repress the *Saccharomyces cerevisiae SER3* gene. *Nature* **429:** 571–574.

Martens JA, Wu PY, Winston F. 2005. Regulation of an intergenic transcript controls adjacent gene transcription in *Saccharomyces cerevisiae*. *Genes Dev* **19:** 2695–2704.

Meaux S, van Hoof A. 2006. Yeast transcripts cleaved by an internal ribozyme provide new insight into the role of the cap and poly(A) tail in translation and mRNA decay. *RNA* **12:** 1323–1337.

Milligan L, Decourty L, Saveanu C, Rappsilber J, Ceulemans H, Jacquier A, Tollervey D. 2008. A yeast exosome cofactor, Mpp6, functions in RNA surveillance and in the degradation of noncoding RNA transcripts. *Mol Cell Biol* **28:** 5446–5457.

Mitchell P, Petfalski E, Tollervey D. 1996. The 3′ end of yeast 5.8S rRNA is generated by an exonuclease processing mechanism. *Genes Dev* **10:** 502–513.

Mitchell P, Petfalski E, Shevchenko A, Mann M, Tollervey D. 1997. The exosome: a conserved eukaryotic RNA processing complex containing multiple 3′→5′ exoribonucleases. *Cell* **91:** 457–466.

Murakami H, Goto DB, Toda T, Chen ES, Grewal SI, Martienssen RA, Yanagida M. 2007. Ribonuclease activity of Dis3 is required for mitotic progression and provides a possible link between heterochromatin and kinetochore function. *PLoS One* **2:** e317.

Ojeda L, Keller G, Muhlenhoff U, Rutherford JC, Lill R, Winge DR. 2006. Role of glutaredoxin-3 and glutaredoxin-4 in the iron regulation of the Aft1 transcriptional activator in *Saccharomyces cerevisiae*. *J Biol Chem* **281:** 17661–17669.

Pedro-Segura E, Vergara SV, Rodriguez-Navarro S, Parker R, Thiele DJ, Puig S. 2008. The Cth2 ARE-binding protein recruits the Dhh1 helicase to promote the decay of succinate dehydrogenase *SDH4* mRNA in response to iron deficiency. *J Biol Chem* **283:** 28527–28535.

Puig S, Askeland E, Thiele DJ. 2005. Coordinated remodeling of cellular metabolism during iron deficiency through targeted mRNA degradation. *Cell* **120:** 99–110.

Pujol-Carrion N, Belli G, Herrero E, Nogues A, de la Torre-Ruiz MA. 2006. Glutaredoxins Grx3 and Grx4 regulate nuclear localisation of Aft1 and the oxidative stress response in *Saccharomyces cerevisiae*. *J Cell Sci* **119(Pt 21):** 4554–4564.

Rutherford JC, Ojeda L, Balk J, Muhlenhoff U, Lill R, Winge DR. 2005. Activation of the iron regulon by the yeast Aft1/Aft2 transcription factors depends on mitochondrial but not cytosolic iron-sulfur protein biogenesis. *J Biol Chem* **280:** 10135–10140.

Schaeffer D, van Hoof A. 2011. Different nuclease requirements for exosome-mediated degradation of normal and nonstop mRNAs. *Proc Natl Acad Sci* **108:** 2366–2371.

Schaeffer D, Tsanova B, Barbas A, Reis FP, Dastidar EG, Sanchez-Rotunno M, Arraiano CM, van Hoof A. 2009. The exosome contains domains with specific endoribonuclease, exoribonuclease and cytoplasmic mRNA decay activities. *Nat Struct Mol Biol* **16:** 56–62.

Schmidt K, Xu Z, Mathews DH, Butler JS. 2012. Air proteins control differential TRAMP substrate specificity for nuclear RNA surveillance. *RNA* **18:** 1934–1945.

Schneider C, Leung E, Brown J, Tollervey D. 2009. The N-terminal PIN domain of the exosome subunit Rrp44 harbors endonuclease activity and tethers Rrp44 to the yeast core exosome. *Nucleic Acids Res* **37:** 1127–1140.

Smith SB, Kiss DL, Turk E, Tartakoff AM, Andrulis ED. 2011. Pronounced and extensive microtubule defects in a *Saccharomyces cerevisiae DIS3* mutant. *Yeast* **28:** 755–769.

Tomecki R, Kristiansen MS, Lykke-Andersen S, Chlebowski A, Larsen KM, Szczesny RJ, Drazkowska K, Pastula A, Andersen JS, Stepien PP, et al. 2010. The human core exosome interacts with differentially localized processive RNases: hDIS3 and hDIS3L. *EMBO J* **29:** 2342–2357.

Tong AH, Boone C. 2006. Synthetic genetic array analysis in *Saccharomyces cerevisiae*. *Methods Mol Biol* **313:** 171–192.

Trushina E, McMurray CT. 2007. Oxidative stress and mitochondrial dysfunction in neurodegenerative diseases. *Neuroscience* **145:** 1233–1248.

Tucker M, Valencia-Sanchez MA, Staples RR, Chen J, Denis CL, Parker R. 2001. The transcription factor associated Ccr4 and Caf1 proteins are components of the major cytoplasmic mRNA deadenylase in *Saccharomyces cerevisiae*. *Cell* **104:** 377–386.

van Hoof A, Lennertz P, Parker R. 2000. Yeast exosome mutants accumulate 3′-extended polyadenylated forms of U4 small nuclear RNA and small nucleolar RNAs. *Mol Cell Biol* **20:** 441–452.

van Hoof A, Frischmeyer PA, Dietz HC, Parker R. 2002. Exosome-mediated recognition and degradation of mRNAs lacking a termination codon. *Science* **295:** 2262–2264.

Waldron C, Lacroute F. 1975. Effect of growth rate on the amounts of ribosomal and transfer ribonucleic acids in yeast. *J Bacteriol* **122:** 855–865.

Yamaguchi-Iwai Y, Stearman R, Dancis A, Klausner RD. 1996. Iron-regulated DNA binding by the AFT1 protein controls the iron regulon in yeast. *EMBO J* **15:** 3377–3384.

Yamaguchi-Iwai Y, Ueta R, Fukunaka A, Sasaki R. 2002. Subcellular localization of Aft1 transcription factor responds to iron status in *Saccharomyces cerevisiae*. *J Biol Chem* **277:** 18914–18918.

Zhu C, Byers KJ, McCord RP, Shi Z, Berger MF, Newburger DE, Saulrieta K, Smith Z, Shah MV, Radhakrishnan M, et al. 2009. High-resolution DNA-binding specificity analysis of yeast transcription factors. *Genome Res* **19:** 556–566.